Accounting for intra-molecular vibrational modes in open quantum system description of molecular systems

Jan Roden, Walter T. Strunz, K. Birgitta Whaley, and Alexander Eisfeld

Additional information on J. Chem. Phys.

Accounting for intra-molecular vibrational modes in open quantum system description of molecular systems

Jan Roden,[1,2,a)] Walter T. Strunz,[3] K. Birgitta Whaley,[1] and Alexander Eisfeld[2,4,b)]

[1]*Department of Chemistry, University of California, Berkeley, California 94720, USA*
[2]*Max-Planck-Institut für Physik komplexer Systeme, D-01187 Dresden, Germany*
[3]*Institut für Theoretische Physik, Technische Universität Dresden, D-01062 Dresden, Germany*
[4]*Department of Chemistry and Chemical Biology, Harvard University, Cambridge, Massachusetts 02138, USA*

Electronic-vibrational dynamics in molecular systems that interact with an environment involve a large number of degrees of freedom and are therefore often described by means of open quantum system approaches. A popular approach is to include only the electronic degrees of freedom into the system part and to couple these to a non-Markovian bath of harmonic vibrational modes that is characterized by a spectral density. Since this bath represents both intra-molecular and external vibrations, it is important to understand how to construct a spectral density that accounts for intra-molecular vibrational modes that couple further to other modes. Here, we address this problem by explicitly incorporating an intra-molecular vibrational mode together with the electronic degrees of freedom into the system part and using the Fano theory for a resonance coupled to a continuum to derive an "effective" bath spectral density, which describes the contribution of intra-molecular modes. We compare this effective model for the intra-molecular mode with the method of pseudomodes, a widely used approach in simulation of non-Markovian dynamics. We clarify the difference between these two approaches and demonstrate that the respective resulting dynamics and optical spectra can be very different. © *2012 American Institute of Physics*. [http://dx.doi.org/10.1063/1.4765329]

I. INTRODUCTION

In many problems of chemical and biological physics, large molecules or complexes of interacting molecules are embedded in an environment, e.g., a fluid solvent, protein scaffold, or a surface. Examples are organic dyes in liquid solution and solid state matrices,[1–5] organic semiconductors on surfaces,[6] or chlorophyll molecules in protein complexes (light-harvesting complexes).[7–11] Much of the information about such complex molecular systems is obtained from optical spectroscopy.[3,12–22] However, the interpretation of spectra is often complicated due to the coupling of the electronic excitations of the molecules to the many intra-molecular modes and external vibrational modes of the environment.

To be able to describe these complex electronic-vibrational (vibronic) dynamics, one often makes use of open quantum system approaches, which divide the entire complex into a set of explicitly treated degrees of freedom (DOF), the "system," and a bath of harmonic vibrational modes that are coupled to the system. Two important concerns when using this approach are the choice of which DOF are to be included into the system Hamiltonian and how the bath is modeled, e.g., as Markovian or non-Markovian in its dynamics. (In this paper we refer to a "Markovian bath" when the bath correlation function is a delta function in time, that is, it decays infinitely fast with respect to the relevant

time scales, and a "non-Markovian bath" if not, since the reduced dynamics will be of Lindblad form in the former case.)

In application to molecules embedded in an environment, two primary choices for the system part have been employed. In the first model, which we term the "vibronic system model" (VSM), the system part contains the relevant molecular electronic states together with one or more "important" vibrational modes. The latter are typically the intra-molecular modes (IMs) for individual molecules that couple most strongly to the molecular electronic excitation. These IMs that are explicitly incorporated into the system Hamiltonian are usually described by Born-Oppenheimer (BO) potentials in the different electronic states that are shifted with respect to each other by a shift ΔQ along a vibrational coordinate Q. The vibrational modes in the system are then coupled to a bath of harmonic modes, representing the many other intra-molecular and external vibrational DOF. This coupling is commonly described by the bath spectral density, which expresses the coupling strength as a function of the frequency of the harmonic bath modes. Because of the inclusion of both electronic *and* vibrational DOF into the system part, we refer to this model as the "vibronic system model."

Since the inclusion of vibrational DOF into the system part causes an immense growth of the corresponding system Hilbert space, simulations based on the VSM are usually limited to either a small number of vibrational modes in the system or a small number of interacting molecules and electronic states. Therefore, a second model is widely used in which

the system part contains only the electronic states and the electronic excitation couples to a harmonic bath representing *all* vibrational DOF. We shall refer to this as the "electronic system model" (ESM). Since the bath now also includes the IMs, which couple strongly to the electronic excitation, in the ESM the bath is typically non-Markovian. This is in contrast to the VSM, where the fact that the most strongly coupled modes are incorporated explicitly into the system is often taken to justify a Markovian description of the remaining, more weakly coupled modes.

Although the VSM and the ESM are both widely used, the relation between the two approaches is still not clear in some key respects. One important issue is how to treat IMs that are coupled to additional modes (usually of the environment). In the VSM, it is straightforward to take such IMs into account, since they may be explicitly incorporated into the system as described above. In the ESM, however, it is not *a priori* clear how to implement the IMs in an equivalent manner while retaining the relative simplicity and compact representation of the ESM. Since the system degrees of freedom are characterized by a smaller Hilbert space in the ESM than in the VSM, the ESM is more scalable and hence preferred when carrying out numerical simulations of larger molecular aggregates. Thus, a proper inclusion of IMs in the ESM would be very useful for calculations with large pigment-protein aggregates. Therefore, the goal is to find an "effective" bath spectral density in the ESM that represents the IMs in a form that is equivalent to their explicit incorporation in the VSM. This problem has been addressed in Ref. 23 (see also references therein) for the case of an Ohmic spectral density with exponential cutoff in the VSM.

In the present work, we establish a relation between the ESM and the VSM by proceeding analogously to Fano's treatment of a resonance coupled to a continuum.[24] In particular, we derive a formula for an effective bath spectral density for the ESM that allows IMs to be taken explicitly into account.

We also show how the model for the intra-molecular mode used here is connected to the so-called method of "pseudomodes,"[25–27] (PM) a widely applied concept to describe non-Markovian dynamics (see also Refs. 28–30). We clarify the relation and the difference between the treatment of pseudomodes and the intra-molecular modes within the ESM. We further demonstrate that the difference between the PM and IM models results in qualitatively different dynamics and optical spectra.

The remainder of the paper is organized as follows: In Sec. II we introduce the open system approach, together with the definitions and notations used in the present work. The following Sec. III describes the VSM and ESM approaches to modeling of electronic-vibrational dynamics. In Sec. IV, we establish the connection between the ESM and the VSM, and derive the effective spectral density for the ESM that provides an equivalent representation of the intra-molecular modes. We then clarify in Sec. V the relation between the IM model and the method of pseudo-modes, and compare the dynamics and optical spectra resulting from these two different representations of vibrational modes. We conclude with a summary and an outlook (Sec. VI).

II. GENERAL OPEN SYSTEM APPROACH WITH HARMONIC BATH

Consider a molecule interacting with an environment. The electronic excitation of the molecule is assumed to couple to both the intra-molecular and external vibrational modes. Using the framework of open quantum systems, we write the total Hamiltonian as

$$H_{\text{tot}} = H_{\text{sys}} + H_{\text{int}} + H_{\text{bath}}, \tag{1}$$

that is, as a sum of the system part H_{sys}, the bath H_{bath}, and the interaction H_{int} between system and bath. We will specify the system part later, when we consider the VSM and ESM. The bath

$$H_{\text{bath}} = \sum_{\lambda} \omega_{\lambda} a_{\lambda}^{\dagger} a_{\lambda} \tag{2}$$

is assumed to be a set of harmonic modes with frequencies ω_{λ} and annihilation (creation) operators a_{λ} ($a_{\lambda}^{\dagger}$). We set $\hbar \equiv 1$ throughout this work.

The interaction between system and bath is given by the sum of products of bath (a_{λ}, $a_{\lambda}^{\dagger}$) and system (L) operators,

$$H_{\text{int}} = \sum_{\lambda} \left(\kappa_{\lambda}^{*} a_{\lambda} L^{\dagger} + \kappa_{\lambda} a_{\lambda}^{\dagger} L \right), \tag{3}$$

with coupling constants κ_{λ}. The system operator L will take different forms for the different specific models we consider in Sec. III.

The magnitude of the coupling to the bath can be encoded in the bath spectral density

$$J(\omega) = \sum_{\lambda} |\kappa_{\lambda}|^{2} \, \delta(\omega - \omega_{\lambda}), \tag{4}$$

which is taken to be a continuous function of the frequency ω. To treat finite temperatures T, we introduce the bath correlation function[31]

$$C(t) = \int_{0}^{\infty} d\omega \, J(\omega) \left(\cos(\omega t) \coth \frac{\omega}{2T} - i \sin(\omega t) \right) \tag{5}$$

(we set the Boltzmann constant k_B to unity) and its Fourier transform

$$C(\omega) = \int_{-\infty}^{\infty} dt \, e^{i\omega t} C(t), \tag{6}$$

which we shall refer to as the "bath correlation spectrum."

It is often useful to calculate $C(\omega)$ directly from $J(\omega)$ (or vice versa), rather than via Eqs. (5) and (6). This can be done via the relation[32]

$$C(\omega) = \left(1 + \coth \left(\frac{\omega}{2T} \right) \right) J^{A}(\omega) \tag{7}$$

with the anti-symmetrized spectral density

$$J^{A}(\omega) = \begin{cases} J(\omega), & \omega \geq 0 \\ -J(-\omega), & \omega < 0. \end{cases} \tag{8}$$

We note that in general $C(\omega)$ is a complicated function leading to non-Markovian dynamics.

III. VIBRONIC AND ELECTRONIC SYSTEM MODELS

A. Vibronic system model

We consider a single molecule embedded in an environment. For simplicity, we take into account only two electronic states of the molecule, namely, the ground state $|g\rangle$ and one excited state $|e\rangle$. We shall also include only a single vibrational mode in the system degrees of freedom. This vibrational mode (the IM) is assumed to be harmonic with the same frequency Ω in both electronic states, so that the two Born-Oppenheimer potentials of the mode in the two electronic states have the same shape. We further assume that the two potentials are shifted with respect to each other in energy by the electronic transition energy ε and are also characterized by a relative shift of ΔQ along the coordinate Q of the vibrational mode (see Fig. 1).

Such a model of shifted harmonic Born-Oppenheimer potentials for the vibrational modes that are explicitly incorporated in the system part is often used in the literature (see, e.g., Refs. 32–34) and was found in many cases to be a reasonable description of these modes (see, e.g., Refs. 35 and 36). The harmonic shape of these potentials will allow us later to establish the connection of the VSM with the ESM.

In the electronic ground state, the vibrational mode has the Hamiltonian

$$H_g = \Omega \, b_g^\dagger b_g \qquad (9)$$

with the annihilation operator $b_g = (Q + iP)/\sqrt{2}$, where Q and P are the dimensionless position and momentum operators of the mode. In the excited electronic state, located at energy ϵ above the ground state, we have

$$H_e = \varepsilon + \Omega \, b_e^\dagger b_e, \qquad (10)$$

where b_e is the annihilation operator for the mode's potential in the excited electronic state. The latter is shifted by the dimensionless excited-state displacement ΔQ, so that $b_e = ((Q - \Delta Q) + iP)/\sqrt{2}$. The excited state annihilation operator is related to the ground state annihilation operator b_g by a simple shift:

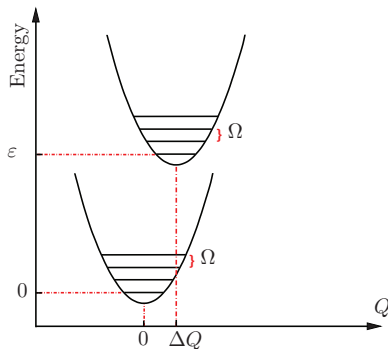$$b_e = b_g - \sqrt{X}, \qquad (11)$$

FIG. 1. Harmonic Born-Oppenheimer potentials of a single vibrational mode with coordinate Q in the two electronic states. The frequency of the mode is given by Ω and the potentials are shifted with respect to each other by ε in energy and by ΔQ along the coordinate Q.

where

$$X = (\Delta Q)^2/2 \qquad (12)$$

is the so-called Huang-Rhys factor,[37] which quantifies the strength with which the electronic excitation couples to the vibrational mode.

The system part H_{sys} of the total Hamiltonian in Eq. (1) is thus given by

$$H_{\text{sys}}^{\text{VSM}} = H_g|g\rangle\langle g| + H_e|e\rangle\langle e|, \qquad (13)$$

which, using Eqs. (9)–(11), can be written as

$$H_{\text{sys}}^{\text{VSM}} = (\varepsilon + \Omega X)|e\rangle\langle e| - \Omega\sqrt{X}|e\rangle\langle e|(b_g^\dagger + b_g)$$
$$+ \Omega \, b_g^\dagger b_g. \qquad (14)$$

From Eq. (14), one sees that the model of the two oscillators shifted with respect to each other in ground and excited states, described here, amounts to a single oscillator that couples linearly (see second term) to the electronic excitation.

For the coupling to the bath, defined in Eq. (3), we use a model analogous to the one described in Ref. 33. For the ground state oscillator, the coupling to the bath is via the coordinate Q, whereas for the (shifted) excited state oscillator it is via the (shifted) coordinate $Q_e = Q - \Delta Q$. Accordingly, we take for the coupling (system) operator L in Eq. (3), the operator

$$L^{\text{VSM}} = |g\rangle\langle g|b_g + |e\rangle\langle e|b_e \qquad (15)$$

$$= b_g - |e\rangle\langle e|\sqrt{X}. \qquad (16)$$

That is, in the electronic ground state the IM couples with the IM annihilation operator b_g to the bath, whereas in the excited electronic state it couples with the displaced IM operator $b_e = b_g - \sqrt{X}$, as a result of the potential shift in the excited state.

The results of the present paper rely on the specific form chosen for the system-bath coupling. In other works, e.g., Refs. 23 and 34, see also Chapter 8 of Ref. 32, different coupling Hamiltonians for the coupling of a vibrational mode or reaction coordinate to a bath are used. In particular, also the form $\sum_\lambda (\kappa_\lambda^2 Q^2/(2\omega_\lambda) - \kappa_\lambda q_\lambda Q)$ for the coupling between the coordinate Q of the system mode and the coordinates q_λ of the bath modes that appears in the so-called Caldeira-Leggett Hamiltonian is widely applied.[32,38]

B. Electronic system model

The vibronic system model, described in Sec. III A, has the drawback that the Hilbert space of the system part grows rapidly as the number of explicitly incorporated vibrational modes or the number of interacting molecules/electronic states is increased. To avoid this, the ESM is widely used (see, e.g., Refs. 7 and 39–42). Here, the system degrees of freedom contain only the electronic DOF and all vibrational DOF are incorporated in the bath to which the electronic excitation couples.

For the description of the ESM, we consider again a molecule embedded in an environment, as in Sec. III A for the VSM. As in the VSM, we take only two electronic states

into account. The system part contains only the two electronic states, so that the system Hamiltonian reads

$$H_{\text{sys}}^{\text{ESM}} = \varepsilon_0 |g\rangle\langle g| + \varepsilon |e\rangle\langle e|, \qquad (17)$$

with the energy ε_0 of the ground state (which we set to zero from now on) and the energy ε of the excited electronic state.

The transition between the two states couples linearly to the harmonic bath. We describe this by taking

$$L^{\text{ESM}} \equiv -|e\rangle\langle e| \qquad (18)$$

for the system coupling operator L in Eq. (3). Note that this model of linear coupling between the electronic projector $|e\rangle\langle e|$ and an implicitly infinite number of bath modes is equivalent to taking infinite dimensional harmonic BO surfaces (instead of the harmonic bath) in ground and excited electronic states that are shifted with respect to each other in each dimension, with shifts proportional to the corresponding coupling constant κ_λ in Eq. (3). This equivalence can be shown by a reformulation of the total Hamiltonian H_{tot} (for an infinite number of modes) that is analogous to the reformulation of $H_{\text{sys}}^{\text{VSM}}$ done in Eq. (14) in Sec. III A for a single IM.

The rest of the model is as described in Sec. II for the general harmonic bath model. Thus, we use the bath correlation spectrum $C(\omega)$ of Eq. (6) (or the spectral density $J(\omega)$ in Eq. (4)) to describe the coupling of the electronic excitation to intra-molecular and external vibrational modes, which together are represented by the harmonic bath.

IV. CONNECTION BETWEEN VIBRONIC AND ELECTRONIC SYSTEM MODEL

We show here how a quantitative relation between the VSM and the ESM can be established. In particular, we shall address the question how a damped intra-molecular vibrational mode, which within the VSM is explicitly incorporated into the system part (Sec. III A), can be equivalently described within the ESM. It will be shown that this is possible by taking an "effective" spectral density $J_{\text{ESM}}(\omega)$ in the ESM, which can be calculated from the spectral density $J_{\text{VSM}}(\omega)$ to which the system vibrational mode couples within the VSM description.

A. Diagonalization of the bath

We start by considering the total Hamiltonian for the VSM, with the single IM incorporated in the system part. From Eqs. (2), (3), (14), (16), and (17), we see that it can be written as

$$H_{\text{tot}}^{\text{VSM}} = \tilde{H}_{\text{sys}}^{\text{ESM}} + H_{\text{vib}}$$

$$- \sqrt{X}|e\rangle\langle e|\left(\Omega b_g + \sum_\lambda \kappa_\lambda^* a_\lambda + \text{h.c.}\right), \quad (19)$$

where

$$\tilde{H}_{\text{sys}}^{\text{ESM}} \equiv H_{\text{sys}}^{\text{ESM}} + \Omega X |e\rangle\langle e| \qquad (20)$$

and

$$H_{\text{vib}} \equiv \Omega b_g^\dagger b_g + \sum_\lambda \omega_\lambda a_\lambda^\dagger a_\lambda + \sum_\lambda \left(\kappa_\lambda^* a_\lambda b_g^\dagger + \text{h.c.}\right). \quad (21)$$

In Eq. (19) the electronic projector $|e\rangle\langle e|$ couples linearly to all bath modes a_λ and to the single mode b_g, which are all comprised in H_{vib}. This form is similar to the ESM described before, however, with the difference that within H_{vib} the single mode b_g is coupled to the other modes a_λ (see Eq. (21)), in contrast to the bath of normal modes used in the ESM. Therefore, to find the effective spectral density $J_{\text{ESM}}(\omega)$ for the ESM, we will diagonalize H_{vib} by means of a unitary transformation S so that all modes will be uncoupled. To this end, we define a vector operator $\bar{a}$ with components b_g and $\{a_\lambda\}$, i.e., the annihilation operators of *all* vibrational modes:

$$\bar{a} = (b_g, a_1, \ldots, a_N)^T, \qquad (22)$$

where $\lambda = 1, 2, \ldots, N$ and $(\cdots)^T$ denotes the transpose. Then we can write

$$H_{\text{vib}} = \bar{a}^\dagger M \bar{a}, \qquad (23)$$

with

$$M = \begin{pmatrix} \Omega & \kappa_1^* & \kappa_2^* & \cdots & \kappa_N^* \\ \kappa_1 & \omega_1 & 0 & \cdots & 0 \\ \kappa_2 & 0 & \omega_2 & \ddots & \vdots \\ \vdots & \vdots & \ddots & \ddots & 0 \\ \kappa_N & 0 & \cdots & 0 & \omega_N \end{pmatrix}. \qquad (24)$$

It is convenient to also introduce a vector that contains all the couplings:

$$\bar{\kappa} \equiv \sqrt{X}(\Omega, \kappa_1, \ldots, \kappa_N)^T. \qquad (25)$$

The total Hamiltonian can then be written as

$$H_{\text{tot}}^{\text{VSM}} = \tilde{H}_{\text{sys}}^{\text{ESM}} + \bar{a}^\dagger M \bar{a} - |e\rangle\langle e|(\bar{\kappa}^\dagger \bar{a} + \bar{a}^\dagger \bar{\kappa}). \quad (26)$$

We now diagonalize M by means of a unitary transformation S, i.e.,

$$D \equiv S M S^\dagger \qquad (27)$$

is a diagonal matrix that contains the eigenvalues of M. The total Hamiltonian now reads

$$H_{\text{tot}}^{\text{VSM}} = \tilde{H}_{\text{sys}}^{\text{ESM}} + \bar{c}^\dagger D \bar{c} - |e\rangle\langle e|(\bar{v}^\dagger \bar{c} + \bar{c}^\dagger \bar{v}), \qquad (28)$$

where we have introduced

$$\bar{c} \equiv S \bar{a}, \qquad (29)$$

with $\bar{c} = (c_0, c_1, \ldots, c_N)^T$ and

$$\bar{v} \equiv S \bar{\kappa}, \qquad (30)$$

with $\bar{v} = (v_0, v_1, \ldots, v_N)^T$. Denoting the eigenvalues of M by ξ_ρ, we can write

$$H_{\text{tot}}^{\text{VSM}} = \tilde{H}_{\text{sys}}^{\text{ESM}} + \sum_\rho \xi_\rho c_\rho^\dagger c_\rho - |e\rangle\langle e| \sum_\rho \left(v_\rho^* c_\rho + v_\rho c_\rho^\dagger\right), \qquad (31)$$

where $\rho = 0, 1, \ldots, N$. The new couplings can be calculated from $v_\rho = (S\bar{\kappa})_\rho$, where S is the matrix consisting of the eigenvectors of M. Comparison with Eqs. (1)–(4), (17) and (18) implies that Eq. (31) corresponds to an ESM with spectral density

$$J_{\mathrm{ESM}}(\omega) = \sum_\rho |v_\rho|^2 \, \delta(\omega - \xi_\rho). \qquad (32)$$

Note that because of the appearance of the shifted electronic Hamiltonian $\tilde{H}_{\mathrm{sys}}^{\mathrm{ESM}}$ instead of the original electronic Hamiltonian $H_{\mathrm{sys}}^{\mathrm{ESM}}$ in Eq. (31), in addition to requiring the new effective spectral density, we also need to now add an energy ΩX to the excited electronic state (Eq. (20)). From the above formulation one sees that the effective spectral density $J_{\mathrm{ESM}}(\omega)$ for the ESM of Eq. (32) can be obtained by diagonalizing the matrix M.

The elements of M are determined by the VSM spectral density

$$J_{\mathrm{VSM}}(\omega) = \sum_\lambda |\kappa_\lambda|^2 \delta(\omega - \omega_\lambda) \qquad (33)$$

and by the frequency Ω of the single mode that was incorporated into the system part. The new bath frequencies are given by the eigenvalues ξ_ρ of M and the corresponding couplings v_ρ are calculated via the transformation in Eq. (30) (where the coupling X to the single mode enters, cf. Eqs. (25) and (30)).

This diagonalization can be done numerically, which we will use to verify the analytical results presented below. Starting from a spectral density $J_{\mathrm{VSM}}(\omega)$ that is a continuous function of ω, we can obtain the discrete couplings κ_λ from the values of $J_{\mathrm{VSM}}(\omega_\lambda)$ at discrete frequencies ω_λ via a simple quadrature:

$$\kappa_\lambda = \sqrt{J_{\mathrm{VSM}}(\omega_\lambda) \, \Delta\omega_\lambda}, \qquad (34)$$

with finite frequency intervals $\Delta\omega_\lambda = (\omega_{\lambda+1} - \omega_{\lambda-1})/2$ (and defining $\Delta\omega_1 = \omega_2 - \omega_1$ and $\Delta\omega_N = \omega_N - \omega_{N-1}$ at the boundaries). After the diagonalization, the inverse procedure is undertaken to obtain the values $J_{\mathrm{ESM}}(\xi_\rho)$ of the corresponding spectral density for the ESM at the discrete frequencies ξ_ρ, by explicitly calculating

$$J_{\mathrm{ESM}}(\xi_\rho) = |v_\rho|^2 / \Delta\xi_\rho. \qquad (35)$$

The finite intervals $\Delta\xi_\rho$ are obtained analogously to the $\Delta\omega_\lambda$, but now using the eigenvalues ξ_ρ instead of ω_λ.

B. Treatment analogous to Fano's approach

From the form of the matrix M in Eq. (24), we see that this formulation of the system IM coupled to a bath of harmonic modes is equivalent to the problem of a resonance coupled to a continuum that was first considered by Fano in 1935. In particular, rewriting the spectral density as[43]

$$J_{\mathrm{ESM}}(\omega) = \sum_\rho |v_\rho|^2 \delta(\omega - \xi_\rho) \qquad (36)$$

$$= \frac{1}{\pi} \sum_\rho \mathrm{Im} \, \frac{|v_\rho|^2}{\xi_\rho - (\omega + i\epsilon)}, \qquad (37)$$

one sees that one can proceed completely analogously to the treatment in Refs. 24 and 43 for a single resonance coupled to one continuum (where our matrix M and vector $\bar{\kappa}$ in Eqs. (24) and (25) correspond, respectively, to the matrix H and vector $|M\rangle$ in Ref. 43). We thereby obtain the following form for the effective spectral density $J_{\mathrm{ESM}}(\omega)$:

$$J_{\mathrm{ESM}}(\omega) = \frac{X \, \omega^2 \, J_{\mathrm{VSM}}(\omega)}{\pi^2 (J_{\mathrm{VSM}}(\omega))^2 + (\omega - \Omega - F(\omega))^2}. \qquad (38)$$

Here, $F(\omega)$ is given by the principal value integral

$$F(\omega) \equiv \mathcal{P} \int_{-\infty}^{+\infty} dE \, \frac{J_{\mathrm{VSM}}(E)}{\omega - E}. \qquad (39)$$

Using this result, the effective spectral density $J_{\mathrm{ESM}}(\omega)$ for the ESM can now be readily calculated for a broad range of different VSM spectral densities $J_{\mathrm{VSM}}(\omega)$. It should be noted that the coupling X to the single mode, which is explicitly incorporated into the system part within the VSM, appears in Eq. (38) simply as a global scaling factor (cf. Eqs. (25), (30) and (32)).

C. Special cases of spectral densities

In the following we will consider two commonly applied special cases for the spectral density (SD) $J_{\mathrm{VSM}}(\omega)$ for the VSM. First, we consider the case where the single vibrational mode in the system part (i.e., the IM) couples to a constant spectral density, which for zero temperature corresponds to a Markovian bath, i.e., to a bath correlation function that is a delta function in time. Second, we consider the case where the IM couples to an Ohmic spectral density with an exponential cutoff. For these two examples, we have confirmed that the effective spectral densities $J_{\mathrm{ESM}}(\omega)$, calculated via the Fano approach, are in perfect agreement with those calculated by direct numerical diagonalization of the matrix M.

1. Constant spectral density

We take a constant spectral density

$$J_{\mathrm{VSM}}(\omega) = \gamma/\pi, \qquad (40)$$

where γ is the damping rate of the single vibrational mode (the strength of the coupling to the bath). Inserting this constant $J_{\mathrm{VSM}}(\omega)$ into the formula Eq. (38), we get

$$J_{\mathrm{ESM}}(\omega) = \frac{1}{\pi} \frac{X \gamma \, \omega^2}{(\omega - \Omega)^2 + \gamma^2}, \qquad (41)$$

since the principal value integral $F(\omega)$ in Eq. (39) gives zero. The resulting spectral density of the ESM in Eq. (41) is a Lorentzian centered at Ω, which is multiplied by the function ω^2. (Note that often a different definition for the spectral density is used that excludes the factor ω^2,[31] that is, $\tilde{J}(\omega) = J(\omega)/\omega^2$; this would merely change Eq. (41) to a simple Lorentzian.) Figure 2 shows the behavior of $J_{\mathrm{ESM}}(\omega)$ for four different values of the frequency Ω of the single mode of the VSM, namely, $\Omega = 5, 10, 15, 20$ (thin solid (red) curves). The maximum of the curves increases with increasing Ω. The underlying constant spectral density $J_{\mathrm{VSM}}(\omega)$

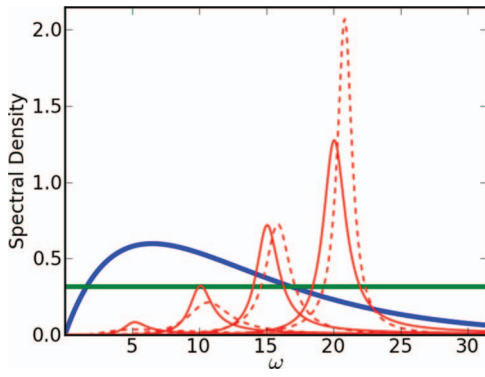FIG. 2. Effective spectral densities $J_{ESM}(\omega)$ for the ESM, calculated for the two special cases of a constant spectral density $J_{VSM}(\omega)$ and an Ohmic spectral density with exponential cutoff for the VSM. The chosen constant spectral density $J_{VSM}(\omega)$ is shown as the thick green solid line given by $J_{VSM}(\omega) = \gamma/\pi$, where we have chosen $\gamma = 1$ (see Eq. (40)). For this case of a constant SD, the resulting spectral density $J_{ESM}(\omega)$ for the ESM is shown for four different values $\Omega = 5, 10, 15, 20$ of the frequency of the single mode of the VSM (thin red solid lines). The maximum of each curve is approximately located at the corresponding value of Ω. For the case of the Ohmic spectral density with exponential cutoff, thick blue solid line, with $\eta = 0.25$ and $\Lambda = 6.5$ (see Eq. (42)), the resulting effective spectral densities $J_{ESM}(\omega)$, are shown for the same four values of Ω as the thin red dashed lines. (The maximum position of the dashed lines increases similarly with increasing Ω.) In all cases we have chosen a Huang-Rhys factor of $X = 0.01$ for the single mode in the VSM. The effective spectral densities $J_{ESM}(\omega)$ are calculated from Eqs. (41) and (45). All energies (ω, Ω, γ, Λ) and the spectral density are given in the same (arbitrary) units.

$= \gamma/\pi$ is shown in Fig. 2 as the thick solid (green) line and we have chosen a coupling strength of $\gamma = 1$ in all of these calculations. For each of the red curves, the maximum is approximately located at the corresponding frequency Ω. It is important to note that the curves have an asymmetric shape; towards high energies their tail converges to the constant ($X\gamma/\pi$) as $\omega \to +\infty$ (we have chosen $X = 0.01$ so that they converge to $0.01/\pi$) and for $\omega \to +0$ they go to zero (see Eq. (41)). This means that for high energies, the effective bath for the ESM gets a constant character, resulting from the underlying constant SD taken in the VSM. These properties of the effective spectral density will change in the following, when we consider a VSM spectral density of Ohmic form with an exponential cutoff.

2. Ohmic spectral density with exponential cutoff

As an example of a more realistic spectral density, which is zero for $\omega \leq 0$ and falls off at higher energies, we consider an Ohmic spectral density with exponential cutoff

$$J_{VSM}(\omega) = \eta\,\omega\,e^{-\omega/\Lambda}\,\Theta(\omega) \qquad (42)$$

(where $\Theta(\omega)$ denotes the unit step function, which is 1 for $\omega > 0$ and 0 otherwise). This form is frequently used in the literature, e.g., in studies of electronic energy transport for light harvesting systems.[36] We note that this spectral density was already considered in Ref. 23, although different assumptions regarding the coupling to the bath in the VSM were made in that work and the cutoff Λ taken to infinity, resulting in a different expression for the effective spectral density of the ESM compared to the one obtained here (see Eq. (45)). For

the spectral density in Eq. (42), the principal value integral $F(\omega)$ in Eq. (39) yields

$$F(\omega) = \eta(\omega\,e^{-\omega/\Lambda}\,\text{Ei}(\omega/\Lambda) - \Lambda), \qquad (43)$$

where $\text{Ei}(x)$ denotes the exponential integral defined as the principal value integral

$$\text{Ei}(x) \equiv \mathcal{P}\int_{-x}^{+\infty} dy\,e^{-y}/y. \qquad (44)$$

Inserting Eqs. (42) and (43) into the formula in Eq. (38) results in

$$J_{ESM}(\omega) = \qquad\qquad\qquad\qquad\qquad\qquad (45)$$

$$\frac{X\,\eta\,\omega^3\,e^{-\omega/\Lambda}\,\Theta(\omega)}{\pi^2\eta^2\omega^2e^{-2\omega/\Lambda} + (\omega - \Omega + \eta\Lambda - \eta\,\omega\,e^{-\omega/\Lambda}\,\text{Ei}(\omega/\Lambda))^2}.$$

This resulting ESM effective spectral density is also shown in Fig. 2 (thin red dashed lines) for the four frequencies $\Omega = 5, 10, 15, 20$ of the single mode (same values of Ω as for the constant SD considered above). The underlying Ohmic spectral density with exponential cutoff $J_{VSM}(\omega)$ of Eq. (42) is shown as the thick blue solid curve, where we have chosen $\eta = 0.25$ and $\Lambda = 6.5$. The Huang-Rhys factor of the single mode is again $X = 0.01$, as for the constant SD considered before. The resulting curves for $J_{ESM}(\omega)$ differ from the curves obtained for the constant SD (thin red solid lines). In particular, their maxima lie at slightly higher energies and not at the frequencies Ω. Furthermore, the width of the peaks depends on where the peaks lie with respect to the corresponding $J_{VSM}(\omega)$ (blue line). The peak with $\Omega = 20$ is narrower than the corresponding peak for the constant SD (solid line), since at this energy, the Ohmic spectral density with exponential cutoff is below the constant spectral density, that is, the coupling to the bath is weaker. For the peak with $\Omega = 15$, however, the coupling to the bath is of approximately the same strength for both cases (the green and blue curve intersect in this region) and thus the two resulting peaks of the corresponding effective spectral densities have approximately the same width. Accordingly, for the peaks with $\Omega = 5$ and $\Omega = 10$, where the blue curve is above the constant green line, the dashed peaks are broader than the corresponding peaks for the constant SD. This shows, as anticipated, that the effective spectral density $J_{ESM}(\omega)$ depends on the local coupling strength of the underlying spectral density $J_{VSM}(\omega)$ in the region where the frequency Ω of the IM lies.

V. RELATION BETWEEN INTRA-MOLECULAR MODES AND PSEUDOMODES

A. Pseudomodes

Another often used formal approach to describe non-Markovian dynamics is the so-called method of pseudomodes (PMs).[25–27] These PMs appear, for example, from a pole decomposition of a given spectral density of the ESM and can be represented equivalently as vibrational modes incorporated into the system part,[25–27] similar to the incorporation of the intra-molecular modes (IMs) in the VSM in Sec. III A. The real part of the pole corresponds to the frequency of a PM, the imaginary part describes the damping by

a Markovian bath, and the weight of the pole corresponds to the Huang-Rhys factor. It is important to note that the only difference between a PM and an IM as described in Sec. III A is that instead of the coupling operator L^{VSM} given in Eq. (16) that results from an IM, the PM is coupled to the bath by the operator[27]

$$L_{PM}^{VSM} = b_g. \qquad (46)$$

This means that in the PM description, the shift ΔQ between the BO potentials in different electronic states is neglected in the coupling to the bath. That is, the vibrational mode included in the system part is assumed to always couple to the bath as if the molecule were in its electronic ground state, regardless whether it is electronically excited or not.

Taking this modified PM coupling to the bath, Eq. (46), and proceeding analogously to Sec. IV A, the calculation of an effective $J_{ESM}(\omega)$ may be carried out as before for an IM. However, since for the PM the coupling to the bath is now via the operator L_{PM}^{VSM} (Eq. (46)) instead of the IM operator L^{VSM} (Eq. (16)), the PM total Hamiltonian is given by

$$H_{tot}^{PM} = \tilde{H}_{sys}^{ESM} + H_{vib} - \sqrt{X}|e\rangle\langle e|(\Omega b_g + \text{h.c.}) \qquad (47)$$

instead of the IM total Hamiltonian H_{tot}^{VSM} in Eq. (19), with $\tilde{H}_{sys}^{ESM}$ and H_{vib} again given by Eqs. (20) and (21). The only difference between Eq. (47) and the IM Hamiltonian of Eq. (19) is that now the coupling terms $(\sum_\lambda \kappa_\lambda^* a_\lambda + \text{h.c.})$ no longer appear in the third term. From this it follows that for the PM, one can proceed equally as for the IM in Sec. IV A, except that after diagonalizing the matrix M (Eq. (24)) for the PM one has to take a different coupling vector

$$\bar{v}^{PM} \equiv S\bar{\kappa}^{PM}, \qquad (48)$$

instead of Eq. (30), with

$$\bar{\kappa}^{PM} \equiv \sqrt{X}(\Omega, 0, \ldots, 0)^T, \qquad (49)$$

instead of Eq. (25). The resulting effective spectral density for an ESM corresponding to the PM is then given by

$$J_{ESM}^{PM}(\omega) = \sum_\rho |v_\rho^{PM}|^2 \delta(\omega - \xi_\rho), \qquad (50)$$

instead of by Eq. (32), where the v_ρ^{PM} are the components of the vector $\bar{v}^{PM}$ of Eq. (48).

In the case when the PM couples to a Markovian bath, that is, to the constant spectral density $J_{VSM}(\omega)$ in Eq. (40), it is well-known[27] that the effective spectral density for the ESM is given by a single Lorentzian

$$J_{ESM}^{PM}(\omega) = \frac{1}{\pi}\frac{X\gamma\Omega^2}{(\omega - \Omega)^2 + \gamma^2}, \qquad (51)$$

centered at the frequency Ω and with width γ and height proportional to $\Omega^2 X$. Here Ω and X are again the frequency and the coupling of the vibrational mode, in this case the PM, and γ is the strength of the coupling to the Markovian bath. The difference compared to $J_{ESM}(\omega)$ for the IM, given in Eq. (41), is that now the Lorentzian is multiplied by the constant Ω^2 instead by the function ω^2. We have confirmed that the $J_{ESM}^{PM}(\omega)$ given in Eq. (51) is in perfect agreement with the result obtained by numerically diagonalizing the matrix M and calculating $J_{ESM}^{PM}(\omega)$ via Eqs. (48)–(50).

If multiple PMs are incorporated into the system part and each of these is coupled to its own independent Markovian bath, the resulting effective spectral density for the ESM is given by the sum of the corresponding Lorentzians for each PM.

B. Demonstration of differences between PM and IM dynamics

In the following, we will demonstrate that the neglect of the shift ΔQ in the coupling to the bath, that is, the difference between PM and IM, can result in strong differences in wave packet dynamics and in optical spectra. For this, we consider the case of a Markovian bath and zero temperature. This provides a simple, often used model in which the effect of the bath is merely a damping of the vibrational motion in the system and allows a straightforward interpretation of vibrational wave packet dynamics and absorption spectra.

We implement the Markovian bath by taking the bath correlation function

$$C_{markov}(t) = 2\gamma\delta(t), \qquad (52)$$

which, for the case of zero temperature considered here, corresponds to a constant bath spectral density and where γ quantifies the strength of the coupling to the bath.

The dynamics of the system can then be calculated by solving the standard Lindblad master equation[44]

$$\partial_t \rho(t) = -i[H_{sys}, \rho(t)] + \gamma([L\rho, L^\dagger] + [L, \rho L^\dagger]) \qquad (53)$$

for the reduced density operator $\rho(t)$ of the system.

1. Motion of vibrational wave packet

To show the extent of differences in system dynamics that can arise depending on whether the shift ΔQ is taken into account in the coupling to the bath, we look at the motion of a vibrational wave packet in the excited electronic state potential.

We consider the expectation value

$$\langle Q \rangle(t) = \text{tr}(Q\,\rho(t)) \qquad (54)$$

$$= \text{tr}\left((b_g^\dagger + b_g)\rho(t)\right)/\sqrt{2} \qquad (55)$$

of the vibrational coordinate Q, which is obtained from solution of the Lindblad equation, Eq. (53).

We start with the initial state $\rho_0 = |e\rangle\langle e| \otimes |0_g\rangle\langle 0_g|$ in which the molecule is excited electronically and is in the ground vibrational state $|0_g\rangle$ of the electronic *ground state* potential (indicated with the subscript "g"). Thus, we start in the upper potential with a Gaussian wave packet centered at the minimum position of the lower potential (see Fig. 1). This choice is motivated by our subsequent consideration of the absorption spectrum, where we will use the same initial state (see Sec. V B 2 below).

Figure 3 shows resulting trajectories of $\langle Q \rangle$ versus the energy expectation value $\langle E \rangle = \text{tr}(H_{sys}^{VSM} \rho(t))$ and versus time (insets). The excited state BO potential, which is shifted by ΔQ with respect to the ground state potential, is indicated
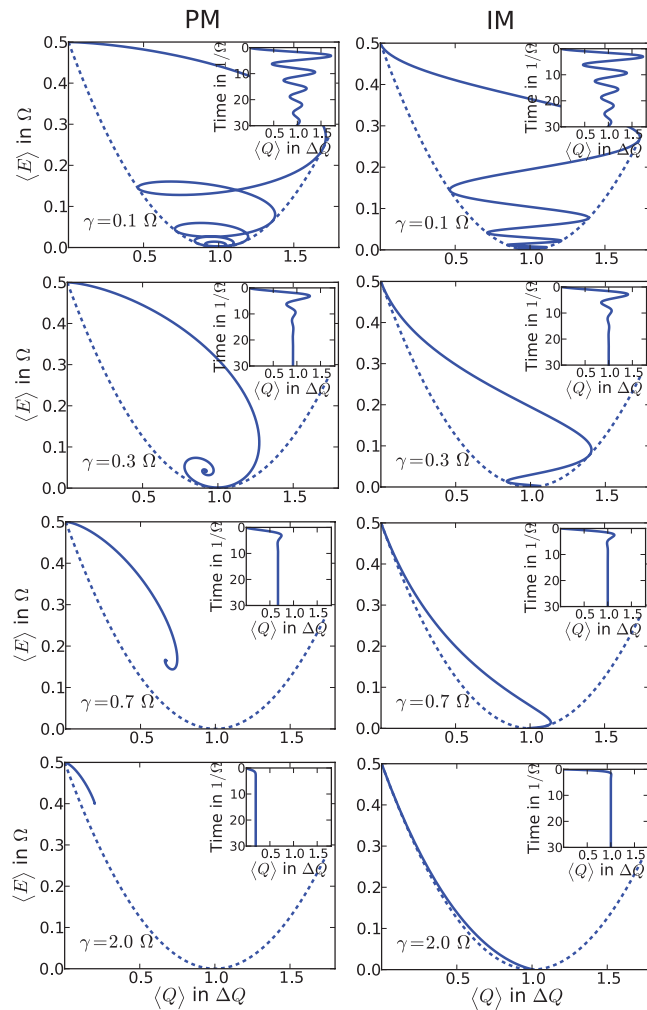
FIG. 3. Motion of the vibrational wave packet (solid line) in the excited electronic state potential (dashed line). The plots show the expectation value $\langle Q \rangle$ of the vibrational coordinate versus the expectation value $\langle E \rangle$ of the energy (and in the inset plot $\langle Q \rangle$ versus time). Left column: the shift ΔQ is ignored in the coupling to the bath (PM). Right column: the shift is taken into account (IM). Results are shown for the initial state $\rho_0 = |e\rangle\langle e| \otimes |0_g\rangle\langle 0_g|$ in which the molecule is electronically excited and in the ground vibrational state of the ground electronic state potential. γ measures the strength of the coupling to the Markovian bath.

in all plots by a dashed line. The left hand panels show the dynamics from the PM approach in which the shift ΔQ is ignored in the coupling to the bath. The right hand panels show the dynamics resulting from the IM approach in which the shift is taken into account. The strength γ of the coupling to the Markovian bath is increased going from top to bottom.

For vanishing coupling strength γ, the two models become identical and describe the free system dynamics without influence of the bath (see Eq. (53)). Therefore, we expect that for a small ratio of $\gamma/\Omega \ll 1$, the difference in the dynamics between the two models will be small, increasing as γ is increased.

This can indeed be observed in Fig. 3. However, even for the smallest value $\gamma = 0.1 \, \Omega$, there are clear differences between the trajectories on the left and right side. For instance, on the left side, the curve of $\langle Q \rangle$ versus $\langle E \rangle$ intersects with itself, whereas on the right side it does not.

The most striking difference between the results shown in left and right panels is the spatial location to which the wave packet of the oscillator in the excited electronic state relaxes. The plots show that for the IM (right hand panels), the wave packet always relaxes towards the minimum position of the *upper* potential, while for the PM (left hand panels) it relaxes more and more towards the minimum position of the *lower* potential (located at zero on the x-axis) as γ is increased. This is because for the PM, due to the neglect of the shift in the system-bath coupling the bath always damps the vibrational motion as if the molecule were in the electronic ground state, so that the system evolves towards the equilibrium position of the ground state potential, regardless of whether it is in the ground or excited electronic state. This damping by the bath becomes stronger as the system-bath coupling strength γ is increased.

2. Absorption

Absorption spectra provide a complementary route for obtaining information about vibrational dynamics. We calculate the absorption spectrum via Fourier transformation of the dipole correlation function

$$D(t) = \mathrm{tr}((\hat{\mu} \otimes \mathbb{1}_{\mathrm{vib}})\rho(t)) \tag{56}$$

(see, e.g., Refs. 45 and 46). Here, $\hat{\mu}$ denotes the transition dipole operator $\hat{\mu} = \mu(|g\rangle\langle e| + |e\rangle\langle g|)$ (we set $\mu \equiv 1$) and $\mathbb{1}_{\mathrm{vib}}$ denotes the unit operator in the space of the vibrational mode of the system.

The dipole correlation function $D(t)$ is calculated by solving the Lindblad equation, Eq. (53), with the initial condition

$$\rho_0 = \hat{\mu}|g\rangle\langle g| \otimes |0_g\rangle\langle 0_g|. \tag{57}$$

Since we consider zero temperature here, the vibrational mode of the system may be taken to be initially in its ground state $|0_g\rangle$ of the electronic ground state BO potential, as before.

In Fig. 4, we show the absorption spectra for the same cases that were considered in Fig. 3. As in Fig. 3, the left hand panels show results from the PM and right hand panels show results from the IM model.

We note first that the peak corresponding to the 0-0 transition in the IM spectra is a narrow line, whereas in the PM spectra it is broadened. Furthermore, for the PM calculations, the entire spectrum, including the 0-0 peak, becomes broader as γ is increased, while for the IM the 0-0 line stays narrow and only the peaks at higher energies become broader.

To explain this, it is convenient to consider the evolution equation

$$\partial_t |\psi(t)\rangle = -i|e\rangle\langle e| \left(H_{\mathrm{sys}}^{\mathrm{VSM}} - i\gamma L^\dagger L \right) |\psi(t)\rangle \tag{58}$$

(corresponding to a Markovian quantum state diffusion description, see, e.g., Ref. 27). For the present case of zero temperature the initial state of the bath is its ground state; this allows us to calculate the dipole correlation function as[27]

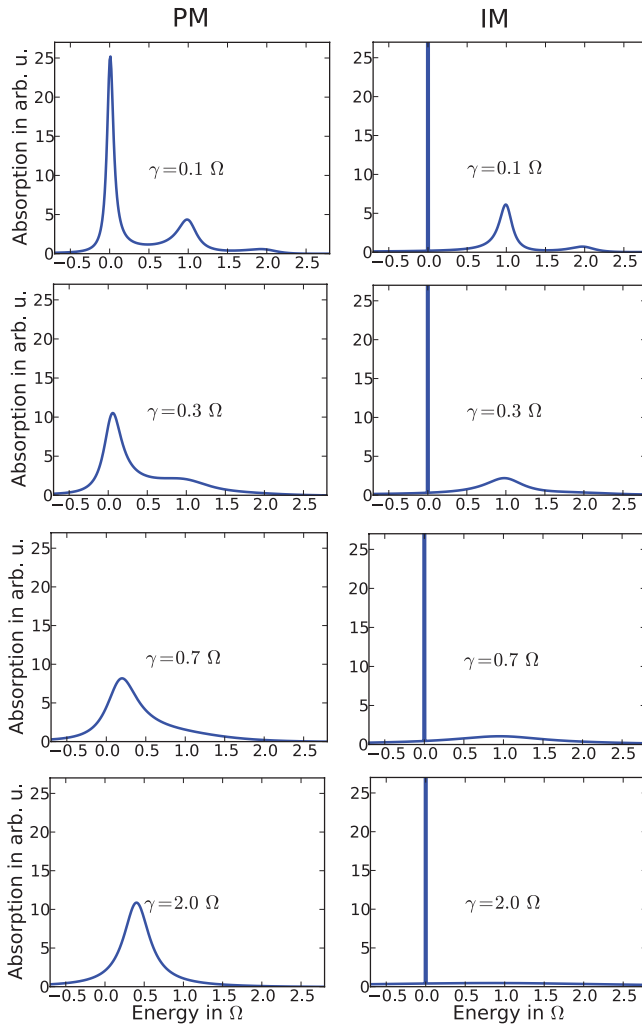$$D(t) = \langle \psi_0 | \psi(t) \rangle \tag{59}$$

PM   IM

FIG. 4. Absorption spectra at zero temperature for the same parameters as in Fig. 3. Left panels: pseudomode (PM) model in which the shift ΔQ is ignored in the coupling to the bath. Right panels: intra-molecular mode (IM) model in which the shift is taken into account. Here, we have taken a Huang-Rhys factor of $X = 0.5$ that corresponds to a shift $\Delta Q = 1$ between the ground and excited state potentials.

with the initial state $|\psi_0\rangle = |e\rangle|0_g\rangle$ (note that we have set $\mu \equiv 1$ for simplicity). The result is equal to that obtained via the Lindblad equation, Eq. (53), and Eqs. (56) and (57). Depending on whether the shift ΔQ is included or neglected in the coupling to the bath, the operator L in Eq. (58) is either given by L^{VSM} or by $L_{\text{PM}}^{\text{VSM}}$ (see Eqs. (15) and (46)).

The initial state $|e\rangle|0_g\rangle$ is the same as the initial state chosen for the wave packet dynamics shown in Fig. 3. For the explanation of the spectra, it is convenient to switch from the wave packet perspective to a representation with respect to eigenstates $|n_e\rangle$ of the harmonic BO potential in the excited electronic state. We expand the initial state $|0_g\rangle$ of the vibrational mode in this basis as

$$|0_g\rangle = \sum_{n_e=0}^{\infty} \langle n_e|0_g\rangle|n_e\rangle, \tag{60}$$

where the amplitudes $\langle n_e|0_g\rangle$ correspond to the Franck-Condon factors $|\langle n_e|0_g\rangle|^2 = e^{-X}X^{n_e}/n_e!$ determined by the Huang-Rhys factor X.

For the IM model, $L = L^{\text{VSM}}$, inserting this expansion into Eq. (58) results in the dipole correlation function

$$D(t) = \sum_{n_e=0}^{\infty} |\langle n_e|0_g\rangle|^2 \, e^{(-i\,\Omega-\gamma)n_e t}. \tag{61}$$

The absorption spectrum is then obtained as a sum of terms corresponding to the individual states $|n_e\rangle$:

$$A(\omega) \propto \sum_{n_e=0}^{\infty} |\langle n_e|0_g\rangle|^2 \frac{n_e\gamma}{(\omega - n_e\Omega)^2 + (n_e\gamma)^2}. \tag{62}$$

Equation (62) shows that each n_e gives a Lorentzian contribution centered at an energy $n_e\Omega$ with an area proportional to $|\langle n_e|0_g\rangle|^2$ and with a width of $n_e\gamma$.

The 0-0 peak, for which $n_e = 0$, is a Lorentzian of zero width, i.e., a delta function at energy zero and with an area proportional to $|\langle 0_e|0_g\rangle|^2 = e^{-X}$—independent of the strength γ of the coupling to the bath, as can be seen in Fig. 4. This is evident from considering the corresponding state $|e\rangle|0_e\rangle$ as initial state in Eq. (58): the right hand side of the equation is zero, showing that this state is stationary and therefore yields a constant term in the dipole correlation function (see Eq. (61) for $n_e = 0$) and accordingly a delta function in the spectrum. This is the state towards which the wave packet relaxes on the right side of Fig. 3.

All higher states $n_e > 0$ decay with a rate $n_e\gamma$, thus generating the broadened peaks at higher energies $n_e\Omega$ in the spectrum.

In contrast, for the PM model, $L = L_{\text{PM}}^{\text{VSM}}$, the state $|e\rangle|0_e\rangle$ is no longer a stationary state of Eq. (58). Consequently, the corresponding 0-0 peak in the spectrum is now broadened, as can be seen in the spectra on the left side of Fig. 4. An analytic expression for the spectrum can be derived also in this situation (see the appendix of Ref. 47).

It is important to note that for finite temperatures the narrow 0-0 line in the IM spectra of Fig. 4 also gains a finite width.

VI. CONCLUSIONS

In this work we have established a relation between several widely used harmonic bath models for molecular systems interacting with an environment. In particular, we considered in detail the relationship between the "electronic system model" (ESM) in which the system part contains only electronic states and all vibrational modes are represented by the bath, and the "vibronic system model" (VSM) in which "important" intra-molecular modes (IMs) are also incorporated into the system part together with the molecular electronic states.

We have obtained a relation between the ESM and the VSM, using a treatment analogous to the one applied by Fano to the problem of a resonance coupled to a continuum. In this way, we showed that it is possible to define an effective bath spectral density for the ESM that is constructively determined by the given underlying bath spectral density of the VSM. This allows one to construct and use an ESM that consistently takes into account key intra-molecular modes and their couplings to the other modes. We demonstrated this relationship

and the equivalence between the two models explicitly for two important special cases of bath spectral densities for the VSM, first, a constant spectral density and second, an Ohmic spectral density with exponential cutoff.

The relation between the ESM and the VSM can be helpful to interpret effective spectral densities obtained from measured spectroscopic data, e.g., from (difference) fluorescence line narrowing spectra[8,13,14] of chromophores interacting with a solvent or protein. Often clear peaks that can be associated with IMs are visible in the spectra. Using the relations discussed in the present work, one can infer information about the interaction of the IMs with the environment and the corresponding relaxation dynamics from the line-shape of these peaks.

In Sec. V, we related the model for the IM to the method of pseudomodes (PMs), which is often applied to describe non-Markovian dynamics in terms of PMs that are incorporated into the system part and coupled to a Markovian bath. We showed that for a Markovian bath, the only difference between the PM and the IM model is that for the PM the shift ΔQ between the Born-Oppenheimer potentials in different electronic states along the vibrational coordinate Q is neglected in the coupling to the Markovian bath, whereas for the IM it is taken into account. We made explicit dynamical calculations to demonstrate that this difference between PM and IM leads to qualitative differences in dynamics and optical spectra. Specifically, we showed that for the IM the peak of the 0-0 transition in the absorption spectrum is a narrow line, whereas for the PM it is broadened, and furthermore, that a vibrational wave packet in the upper BO potential for the IM is damped towards the minimum of that potential, while for the PM it is damped towards the minimum of the *lower* BO potential. Note that this result was derived for a specific coupling of the coordinate Q to the bath (Eq. (3) with $L = b$), which is often used. For other forms of the coupling one can obtain different results.

The methods presented in this work can be used for dynamical description of intra-molecular modes in unified treatments of electronic-vibrational dynamics in extended molecular systems, e.g., in simulations of energy transfer in biological and artificial light-harvesting complexes. To treat these systems, one often uses an approach in which the supramolecular complex is treated as an aggregate consisting of individual "monomers" that contain both the individual chromophores, which interact via electronic resonant excitation exchange, and the local environments of each of these. In such a description the spectral density of single monomers is an important quantity. We note that a straightforward extension of the single molecule treatment to the case of coupled molecules such that the delocalized electronic states interact with *one common* harmonic bath is in general not possible, since for the coupled molecules the assumption of shifted harmonic potential surfaces is no longer valid, and furthermore, non-adiabatic couplings in the excited state have to be taken into account.[48]

The relations established here between the different open quantum system descriptions now allow a consistent comparison of the different approaches and approximations, e.g., non-Markovian approaches that are commonly applied in the framework of the ESM with the more detailed description of electronic-vibrational couplings that are possible within a VSM description. In many situations where a description via (approximative) non-Markovian methods based on the ESM becomes inaccurate or numerically impractical, switching to the VSM description can be useful. For instance, if the effective bath spectral density contains narrow peaks so that the bath correlation function oscillates for a long time, compared to the relevant time scales, resulting in "strongly non-Markovian" dynamics, the approximations applied in an ESM approach may become inaccurate.[27] In such a situation it can be advantageous to switch to the VSM description and to explicitly incorporate the modes that correspond to the sharp peaks in the spectral density into the system part, while the remaining modes are still treated as a Markovian (or weakly non-Markovian) bath.[27] Finally, the VSM can be useful, if one is interested in the explicit dynamics of certain specific vibrational modes, which then can be incorporated into the system part, allowing direct observation of the vibrational or coupled electronic-vibrational dynamics.

ACKNOWLEDGMENTS

[1] A. Nemeth, F. Milota, T. Mančal, V. Lukes, H. F. Kauffmann, and J. Sperling, Chem. Phys. Lett. **459**, 94 (2008).

[2] M. Müller, E. Le Moal, R. Scholz, and M. Sokolowski, Phys. Rev. B **83**, 241203 (2011).

[3] S. Kirstein and S. Daehne, Int. J. Photoenergy **2006**, 20363.

[4] V. Bulović, P. E. Burrows, S. R. Forrest, J. A. Cronin, and M. E. Thompson, Chem. Phys. **210**, 1 (1996).

[5] E. Engel, K. Schmidt, D. Beljonne, J.-L. Brédas, J. Assa, H. Fröb, K. Leo, and M. Hoffmann, Phys. Rev. B **73**, 245216 (2006).

[6] S. R. Forrest, Chem. Rev. **97**, 1793 (1997).

[7] Y.-C. Cheng and G. R. Fleming, Annu. Rev. Phys. Chem. **60**, 241 (2009).

[8] J. Adolphs and T. Renger, Biophys. J. **91**, 2778 (2006).

[9] C. Olbrich, J. Strümpfer, K. Schulten, and U. Kleinekathöfer, J. Phys. Chem. Lett. **2**, 1771 (2011).

[10] G. R. Fleming, G. S. Schlau-Cohen, K. Amarnath, and J. Zaks, Faraday Discuss. **155**, 27 (2012).

[11] S. Shim, P. Rebentrost, S. Valleau, and A. Aspuru-Guzik, Biophys. J. **102**, 649 (2012).

[12] F. C. Spano, J. Am. Chem. Soc. **131**, 4267 (2009).

[13] M. Wendling, T. Pullerits, M. A. Przyjalgowski, S. I. E. Vulto, T. J. Aartsma, R. van Grondelle, and H. van Amerongen, J. Phys. Chem. B **104**, 5825 (2000).

[14] M. Rätsep and A. Freiberg, J. Lumin. **127**, 251 (2007).

[15] A. Telfer, A. A. Pascal, L. Bordes, J. Barber, and B. Robert, J. Phys. Chem. B **114**, 2255 (2010).

[16] T. Brixner, J. Stenger, H. M. Vaswani, M. Cho, R. E. Blankenship, and G. R. Fleming, Nature (London) **434**, 625 (2005).

[17] G. S. Schlau-Cohen, T. R. Calhoun, N. S. Ginsberg, M. Ballottari, R. Bassi, and G. R. Fleming, Proc. Natl. Acad. Sci. U.S.A. **107**, 13276 (2010).

[18] G. S. Schlau-Cohen, A. Ishizaki, and G. R. Fleming, Chem. Phys. **386**, 1 (2011).

[19] N. S. Ginsberg, J. A. Davis, M. Ballottari, Y.-C. Cheng, R. Bassi, and G. R. Fleming, Proc. Natl. Acad. Sci. U.S.A. **108**, 3848 (2011).

[20] D. B. Turner, R. Dinshaw, K.-K. Lee, M. S. Belsley, K. E. Wilk, P. M. G. Curmi, and G. D. Scholes, Phys. Chem. Chem. Phys. **14**, 4857 (2012).

[21] T. Joo, Y. Jia, J.-Y. Yu, M. J. Lang, and G. R. Fleming, J. Chem. Phys. **104**, 6089 (1996).

[22] S. Park, J.-S. Park, and T. Joo, J. Phys. Chem. A **115**, 3973 (2011).

[23] A. Garg, J. N. Onuchic, and V. Ambegaokar, J. Chem. Phys. **83**, 4491 (1985).

[24] U. Fano, Phys. Rev. **124**, 1866 (1961).

[25] B. M. Garraway, Phys. Rev. A **55**, 2290 (1997).

[26] B. J. Dalton, S. M. Barnett, and B. M. Garraway, Phys. Rev. A **64**, 053813 (2001).

[27] J. Roden, W. T. Strunz, and A. Eisfeld, J. Chem. Phys. **134**, 034902 (2011).

[28] A. Imamoğlu, Phys. Rev. A **50**, 3650 (1994).

[29] L. Mazzola, S. Maniscalco, J. Piilo, K.-A. Suominen, and B. M. Garraway, Phys. Rev. A **80**, 012104 (2009).

[30] K. H. Hughes, C. D. Christ, and I. Burghardt, J. Chem. Phys. **131**, 024109 (2009).

[31] V. May and O. Kühn, *Charge and Energy Transfer Dynamics in Molecular Systems* (Wiley VCH, 2000).

[32] S. Mukamel, *Nonlinear Optical Spectroscopy* (Oxford University Press, 1995).

[33] B. Wolfseder and W. Domcke, Chem. Phys. Lett. **235**, 370 (1995).

[34] D. Egorova, M. F. Gelin, M. Thoss, H. Wang, and W. Domcke, J. Chem. Phys. **129**, 214303 (2008).

[35] J. Roden, A. Eisfeld, M. Dvořák, O. Bünermann, and F. Stienkemeier, J. Chem. Phys. **134**, 054907 (2011).

[36] A. Ishizaki, T. R. Calhoun, G. S. Schlau-Cohen, and G. R. Fleming, Phys. Chem. Chem. Phys. **12**, 7319 (2010).

[37] E. S. Medvedev and V. I. Osherov, *Radiationless Transitions in Polyatomic Molecules*, Springer Series in Chemical Physics Vol. 57 (Springer-Verlag, 1995).

[38] U. Kleinekathöfer, J. Chem. Phys. **121**, 2505 (2004).

[39] J. Roden, A. Eisfeld, W. Wolff, and W. T. Strunz, Phys. Rev. Lett. **103**, 058301 (2009).

[40] J. Strümpfer and K. Schulten, J. Chem. Phys. **131**, 225101 (2009).

[41] A. Ishizaki and G. R. Fleming, Proc. Natl. Acad. Sci. U.S.A. **106**, 17255 (2009).

[42] J. Zhu, S. Kais, P. Rebentrost, and A. Aspuru-Guzik, J. Phys. Chem. B **115** 1531 (2011).

[43] S. Glutsch, Phys. Rev. B **66**, 075310 (2002).

[44] G. Lindblad, Commun. Math. Phys. **48**, 119 (1976).

[45] L. Chen, R. Zheng, Q. Shi, and Y. Yan, J. Chem. Phys. **131**, 094502 (2009).

[46] M. Yang, J. Chem. Phys. **123**, 124705 (2005).

[47] J. Roden and A. Eisfeld, J. Chem. Phys. **134**, 034901 (2011).

[48] A. Eisfeld, L. Braun, W. T. Strunz, J. S. Briggs, J. Beck, and V. Engel, J. Chem. Phys. **122**, 134103 (2005).